ANALYZING ENHANCEMENT AND CONTROL OF KERR-NONLINEAR COEFFICIENT IN A THREE-LEVEL V-TYPE INHOMOGENEOUSLY BROADENED ATOMIC MEDIUM

Le Van Doai[a], Dinh Xuan Khoa[a*]

[a]Vinh University, Nghe An, Vietnam
[*]Corresponding author: Email: khoadx@vinhuni.edu.vn

Abstract

The analytical expression for the self-Kerr nonlinear coefficient in a three-level V-type atomic medium is found in the presence of the Doppler effect. Based on the analytical results, we have analyzed the enhancement and control of the Kerr nonlinear coefficient under the condition of electromagnetically induced transparency. It is shown that the Kerr nonlinear coefficient is significantly enhanced around the resonant frequency of both the probe and coupling fields. Simultaneously, the magnitude and sign of the Kerr nonlinear coefficient are controlled with respect to the intensity and frequency of the coupling laser field. The amplitude of the Kerr nonlinear coefficient decreases remarkably as temperature increases (i.e., the Doppler width increases). The analytical model can find potential applications in photonic devices and can explain experimental observations of the Kerr nonlinear coefficient at different temperatures.

Keywords: Analytical model; Electromagnetically induced transparency; Kerr nonlinear effect; Quantum interference and coherence; Three-level V-type atom.

1. INTRODUCTION

It is well known that the Kerr nonlinear coefficient plays an important role in quantum and nonlinear optics. In recent years, a large enhancement of the Kerr nonlinear coefficient with small absorption was obtained through the electromagnetically induced transparency (EIT) effect (Boller et al., 1991), and it has found applications at low-light levels, such as optical Kerr shutters, generation of optical solitons, quantum logic operation, optical bistability (Harris et al.,1990; Harris & Hau, 1995), and others.

The EIT effect has been extensively studied theoretically and experimentally in three-level atomic systems, including lambda-type (Li & Xiao, 1995a), ladder-type (Li & Xiao, 1995b), and V-type (Zhao et al., 2002) configurations. For the three-level lambda-type scheme, the strong coupling field couples the atoms in the lower level of the probe transition. For the three-level ladder-type scheme, the strong coupling field is applied on the upper two unpopulated levels. While for the three-level V-type scheme, the two upper levels are driven by the probe and coupling fields to the common ground state that is initially fully populated. Due to different decay rates in each configuration, the EIT efficiency and the optical properties are different. For a more thorough overview of the EIT effect, the reader can refer to the original references (Bang, Doai, & Khoa, 2019; Fleischhauer et al., 2005).

The first experimental observation of a giant self-Kerr nonlinear coefficient via EIT in a three-level lambda-type inhomogeneously broadened atomic medium was by Wang et al. (2001). They showed that the Kerr nonlinear coefficient is enhanced by several orders of magnitude around the atomic resonant frequency. The experimental results were fit with good agreement by an analytical model (Doai et al., 2015). Recently, many theoretical and experimental studies on the enhancement of Kerr nonlinearity in multilevel atomic systems were also performed (Bang, Khoa et al., 2019; Doai, 2019; Hamedi & Juzeliunas, 2015; Hamedi et al., 2016; Khoa et al., 2014; Sheng et al., 2011).

Although the EIT effect has been studied in all three-level inhomogeneously broadened atomic systems (Li & Xiao, 1995a; Li & Xiao, 1995b; Zhao et al., 2002), the Kerr nonlinearity has so far only been studied in the three-level lambda-type scheme under Doppler broadening. In another context, the three-level V-type configuration associated with the spontaneously generated coherence effect is also of interest for the study of Kerr nonlinearity (Bai et al., 2012; Gao et al., 2016), optical bistability (Anton & Calderon, 2002; Joshi et al., 2003; Li, 2007), group velocity (Bai et al., 2005; Han et al., 2007; Mousavi et al., 2010) and lasing without inversion (Bai et al., 2004). In this work, we develop an analytical model to analyze the enhancement and control of the Kerr nonlinear coefficient in a three-level V-type inhomogeneously broadened atomic medium. The influences of the laser parameters and atomic vapor temperature on the Kerr-nonlinear coefficient are investigated.

2. THEORETICAL MODEL

The three-level V-type atomic medium interacting with two laser fields is depicted in Figure 1. A weak probe laser field with carrier frequency ω_p is applied to the transition $|1\rangle\leftrightarrow|2\rangle$, while a strong coupling laser field with carrier frequency ω_c couples the transition $|1\rangle\leftrightarrow|3\rangle$.
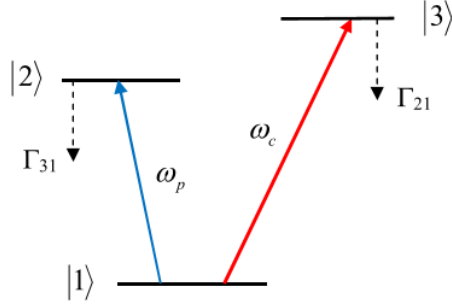

Figure 1. The three-level V-type atomic system

In the dipole and rotating wave approximations, the evolution equation of the density matrix reads:

$$\dot{\rho} = -\frac{i}{\hbar}[H,\rho] + \Lambda\rho , \tag{1}$$

where $\Lambda\rho$ stands for the relaxation processes. The total Hamiltonian of the above system can be given by

$$H = H_{at} + H_{int} , \tag{2}$$

where

$$H_{at} = \hbar\omega_1|1\rangle\langle 1| + \hbar\omega_2|2\rangle\langle 2| + \hbar\omega_3|3\rangle\langle 3| , \tag{3}$$

$$H_{int} = -\frac{\hbar}{2}(\Omega_p e^{-i\Omega_p t}\,|2\rangle\langle 1| + \Omega_c e^{-i\Omega_c t}\,|3\rangle\langle 1|) + c.c., \tag{4}$$

According to the Hamiltonian, the density matrix equations of motion for the system can be written as

$$\dot{\rho}_{11} = \Gamma_{31}\rho_{33} + \Gamma_{21}\rho_{22} + \frac{i}{2}\Omega_p(\rho_{21} - \rho_{12}) + \frac{i}{2}\Omega_c(\rho_{31} - \rho_{13}) , \tag{5}$$

$$\dot{\rho}_{22} = -\Gamma_{21}\rho_{22} + \Gamma_{32}\rho_{33} + \frac{i}{2}\Omega_p(\rho_{12} - \rho_{21}) , \tag{6}$$

$$\dot{\rho}_{33} = -(\Gamma_{31} + \Gamma_{32})\rho_{33} + \frac{i}{2}\Omega_c(\rho_{13} - \rho_{31}), \tag{7}$$

$$\dot{\rho}_{21} = -(\gamma_{21} - i\Delta_p)\rho_{21} + \frac{i}{2}\Omega_p(\rho_{11} - \rho_{22}) - \frac{i}{2}\Omega_c\rho_{23}, \tag{8}$$

$$\dot{\rho}_{23} = -[\gamma_{32} - i(\Delta_p - \Delta_c)]\rho_{23} + \frac{i}{2}\Omega_p\rho_{13} - \frac{i}{2}\Omega_c\rho_{21}, \tag{9}$$

$$\dot{\rho}_{31} = -(\gamma_{31} - i\Delta_p)\rho_{31} + \frac{i}{2}\Omega_c(\rho_{11} - \rho_{33}) - \frac{i}{2}\Omega_p\rho_{32}, \tag{10}$$

The above equations are constrained by $\rho_{11} + \rho_{22} + \rho_{33} = 1$ and $\rho_{mn} = \rho_{nm}^*$. Here, $\Delta_p = \omega_p - \omega_{21}$ and $\Delta_c = \omega_c - \omega_{31}$ are the detuning of the probe and coupling fields, respectively. The Rabi frequencies are given by $\Omega_p = d_{21}E_p/\hbar$ and $\Omega_c = d_{31}E_c/\hbar$ with d_{21} and d_{31} denoting the electric dipole matrix elements. Γ_{mn} is the population relaxation decay rate of the excited state, while $\gamma_{mn} = \Gamma_{mn}/2$ is the coherence atomic decay rate.

In order to derive the analytical expression for the Kerr nonlinear coefficient, we need to solve the density matrix equations up to third-order by using perturbation theory in which each successive approximation is calculated using the density matrix elements of one order less than the one being calculated (Doai et al., 2015). From Equations (5)-(10), we found the solution for the density matrix element ρ_{21} in the first- and third-order perturbations as:

$$\rho_{21}^{(1)} = \frac{i\Omega_p(\rho_{22}^{(0)} - \rho_{11}^{(0)})}{2A}, \tag{11}$$

$$\rho_{21}^{(3)} = -\frac{i\Omega_p}{2A}\frac{\Omega_p^2}{2\Gamma_{21}}\left(\frac{1}{A} + \frac{1}{A^*}\right). \tag{12}$$

where:

$$A = \gamma_{21} - i\Delta_p + \frac{(\Omega_c/2)^2}{\gamma_{32} - i(\Delta_p - \Delta_c)}, \tag{13}$$

and A^* is the complex conjugation of A. The solution of the density matrix element ρ_{21} is calculated up to third order as:

$$\rho_{21} = \rho_{21}^{(1)} + \rho_{21}^{(3)} = \frac{i\Omega_p}{2A} - \frac{i\Omega_p}{2A}\left[\frac{\Omega_p^2}{2\Gamma_{21}}\left(\frac{1}{A} + \frac{1}{A^*}\right)\right]. \tag{14}$$

The total susceptibility of the atomic medium is related to the density matrix element ρ_{21} as follows (Boyd, 2008):

$$\chi = -2\frac{Nd_{21}}{\varepsilon_0 E_p}\rho_{21} \equiv \frac{iNd_{21}^2}{\varepsilon_0 \hbar A} - \left[\frac{iNd_{21}^4}{\varepsilon_0 \hbar^3}\frac{1}{2\Gamma_{21}}\frac{1}{A}\left(\frac{1}{A}+\frac{1}{A^*}\right)\right]E_p^2. \tag{15}$$

The total susceptibility can be written in another way as (Boyd, 2008):

$$\chi = \chi^{(1)} + 3E_p^2 \chi^{(3)}. \tag{16}$$

Comparing Equations (15) and (16) we obtain the first- and third-order susceptibilities as follows:

$$\chi^{(1)} = \frac{iNd_{21}^2}{\varepsilon_0 \hbar}\frac{1}{A}, \tag{17}$$

$$\chi^{(3)} = -\frac{iNd_{21}^4}{3\varepsilon_0 \hbar^3}\frac{1}{2\Gamma_{21}}\frac{1}{A}\left(\frac{1}{A}+\frac{1}{A^*}\right). \tag{18}$$

Now we study the effect of Doppler broadening on the first- and third-order susceptibilities. To eliminate the first-order Doppler effect, we consider the probe and coupling beams co-propagating inside the medium. Therefore, an atom moving with velocity v in the propagation direction of the probe beam will see an upshift frequency of the probe and coupling laser as $\omega_p + (v/c)\omega_p$ and $\omega_c + (v/c)\omega_c$, respectively. Therefore, the susceptibility expressions must be modified to

$$\chi^{(1)}(v)dv = \frac{iN_0 d_{21}^2}{u\sqrt{\pi}\varepsilon_0 \hbar}\frac{e^{-v^2/u^2}}{A(v)}dv, \tag{19}$$

$$\chi^{(3)}(v)dv = -\frac{iN_0 d_{21}^4}{3u\sqrt{\pi}\varepsilon_0 \hbar^3}\frac{e^{-v^2/u^2}}{A(v)}\left[\frac{1}{A(v)}+\frac{1}{A^*(v)}\right]dv, \tag{20}$$

where $u = \sqrt{2k_B T/m}$ is the root mean square atomic velocity, N_0 is the total atomic density of the atomic medium, and

$$A(v) = \gamma_{21} - i\left(\Delta_p + \frac{v}{c}\omega_p\right) + \frac{\Omega_c^2/4}{\gamma_{32} - i(\Delta_p - \Delta_c) - i\frac{v}{c}(\omega_p - \omega_c)}. \tag{21}$$

By integrating (19) and (20) over the velocity v from $-\infty$ to $+\infty$, we have:

$$\chi^{(1)} = \frac{iN_0 d_{21}^2 \sqrt{\pi}}{\varepsilon_0 \hbar (\omega_p u / c)} e^{a^2} [1 - erf(a)] , \tag{22}$$

$$\chi^{(3)} = -\frac{iN_0 d_{21}^4}{3\sqrt{\pi}\varepsilon_0 \hbar^3 (\omega_p u / c)^2} \tag{23}$$

$$\times \left\{ 2\sqrt{\pi} \left(-1 + \sqrt{\pi} a e^{a^2} [1 - erf(a)] \right) + \frac{\pi \left(e^{a^2} [1 - erf(a)] + e^{a^{*2}} [1 - erf(a^*)] \right)}{a + a^*} \right\} ,$$

where

$$a = \frac{c}{\omega_p u} \left(\gamma_{21} - i\Delta_p + \frac{\Omega_c^2 / 4}{\gamma_{32} - i(\Delta_p - \Delta_c)} \right) = \frac{c}{\omega_p u} A , \tag{24}$$

a^* is the complex conjugation of a, and $erf(a)$ is the error function.

From the first- and third-order susceptibilities, we find the expressions for the linear index (n_0) and the Kerr nonlinear coefficient n_2 as (Doai et al., 2015):

$$n_0 = \sqrt{1 + \text{Re}(\chi^{(1)})} , \tag{25}$$

$$n_2 = \frac{3\text{Re}(\chi^{(3)})}{4\varepsilon_0 n_0^2 c} . \tag{26}$$

3.   RESULTS AND DISCUSSION

The theoretical model is applied to ^{87}Rb atomic vapor with the states $|1\rangle$, $|2\rangle$, and $|3\rangle$ chosen as $5S_{1/2}(F = 1)$, $5P_{1/2}(F' = 1)$, and $5P_{1/2}(F' = 2)$, respectively. The atomic parameters are (Doai et al., 2015): $N = 3.5 \times 10^{17}$ atoms/m^3, $\Gamma_{21} = \Gamma_{31} = 6$ MHz, $\gamma_{21} = 3$ MHz, $\gamma_{32} = 6$ MHz, and $d_{21} = 1.6 \times 10^{-29}$ cm.

In Figure 2 we examine the influence of Doppler broadening on the EIT and dispersion spectra by plotting the absorption (dashed line) and dispersion (solid line) coefficients versus probe detuning Δ_p at different temperatures $T = 200$ K (a) and $T = 300$ K (b). The parameters of the coupling field employed in Figure 2 are $\Omega_c = 100$ MHz and $\Delta_c = 0$. It is clear that an increase in temperature leads to the depth and width of the EIT window being significantly reduced. Simultaneously, the amplitude of the normal dispersive curve inside the EIT window is reduced remarkably. We note that due to the decay rate between excited states in the three-level V-type system being much greater than that of three-level lambda-type system, the EIT effect in the V-type system occurs with more intensity of the coupling field.
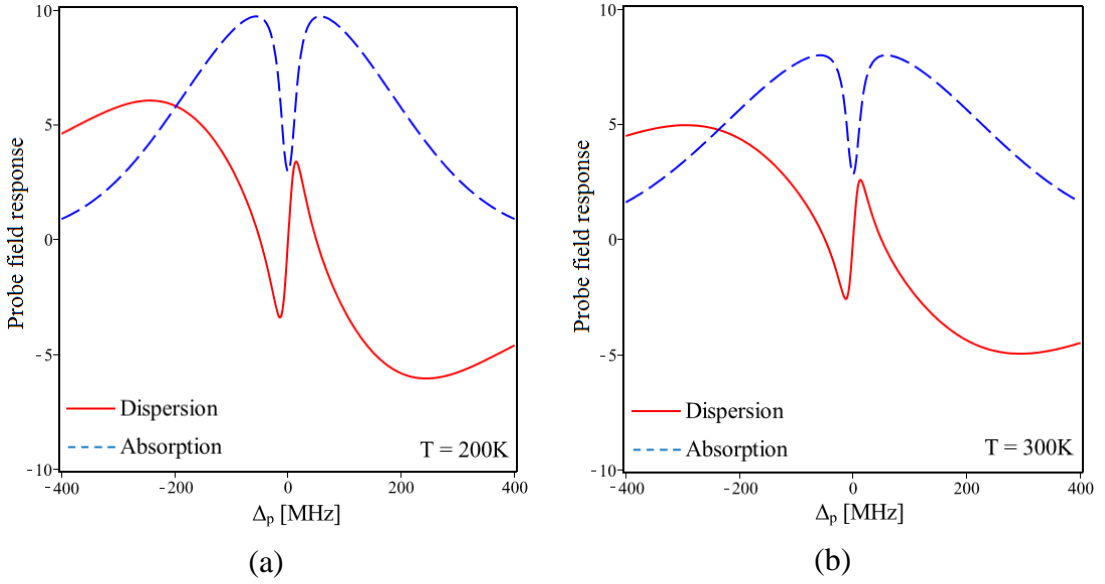
(a) (b)

Figure 2. The absorption (dashed line) and dispersion (solid line) coefficients as functions of probe detuning at temperatures T = 200 K (a) and T = 300 K (b)

Note: The parameters of the coupling field are taken as Ω_c = 100 MHz and $\Delta_c = 0$.
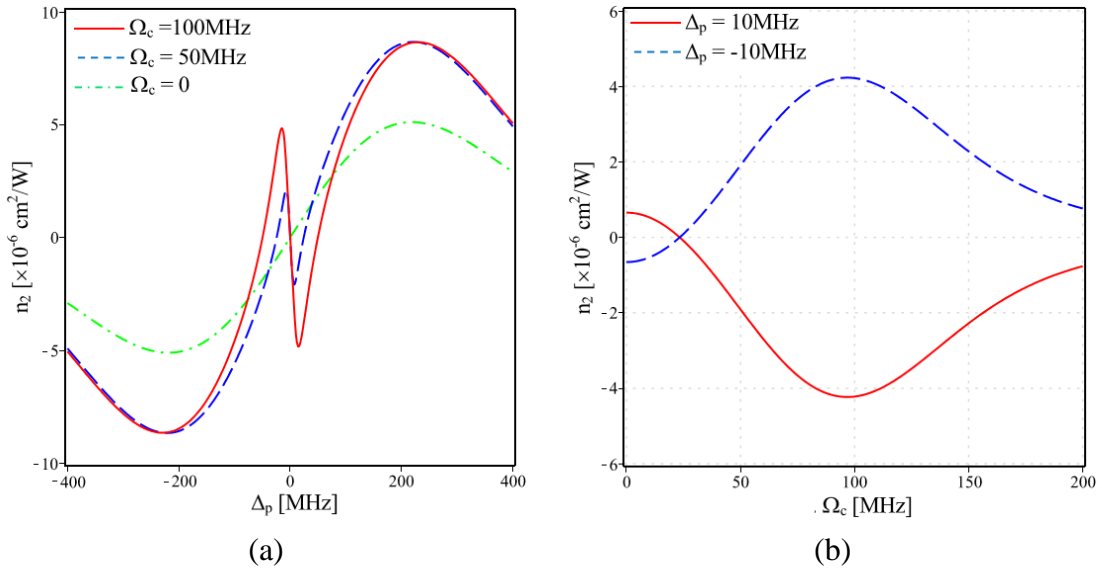

(a) (b)

Figure 3. (a) The Kerr nonlinear coefficient as a function of probe detuning with different values of coupling Rabi frequency Ω_c = 0 (dash-dotted line), Ω_c = 50 MHz (dashed line), and Ω_c = 100 MHz (solid line); (b) The Kerr nonlinear coefficient as a function of coupling Rabi frequency with different values of probe detuning Δ_p = -10 MHz (dashed line) and Δ_p = 10 MHz (solid line)

Note: Other parameters are taken as $\Delta_c = 0$ and T = 300 K.

Now, we analyze the control of the Kerr nonlinear coefficient via the intensity of the coupling field by plotting the Kerr nonlinear coefficient versus probe detuning Δ_p for

various values of the coupling Rabi frequency $\Omega_c = 0$ (dash-dotted line), $\Omega_c = 50$ MHz (dashed line), and $\Omega_c = 100$ MHz (solid line), as shown in Figure 3(a). The variations of the Kerr nonlinear coefficient versus the Rabi frequency of the coupling field when $\Delta_c = 0$, $\Delta_p = 10$ MHz (solid line), $\Delta_p = -10$ MHz (dashed line), and $T = 300$ K are illustrated in Figure 3(b). From Figure 3(a) we can see a fundamental modification and great enhancement of the Kerr nonlinear coefficient inside the EIT window. This means that a normal dispersive curve appears on a line profile of the Kerr nonlinear coefficient accompanied by a pair of negative-positive values of n_2 around the resonant frequency of the probe field $\Delta_p = 0$. By increasing the coupling intensity, the amplitude of this dispersive curve is enhanced considerably. Figure 3(b) shows that the magnitude and sign of the Kerr nonlinear coefficient are changed by adjusting the coupling Rabi frequency.
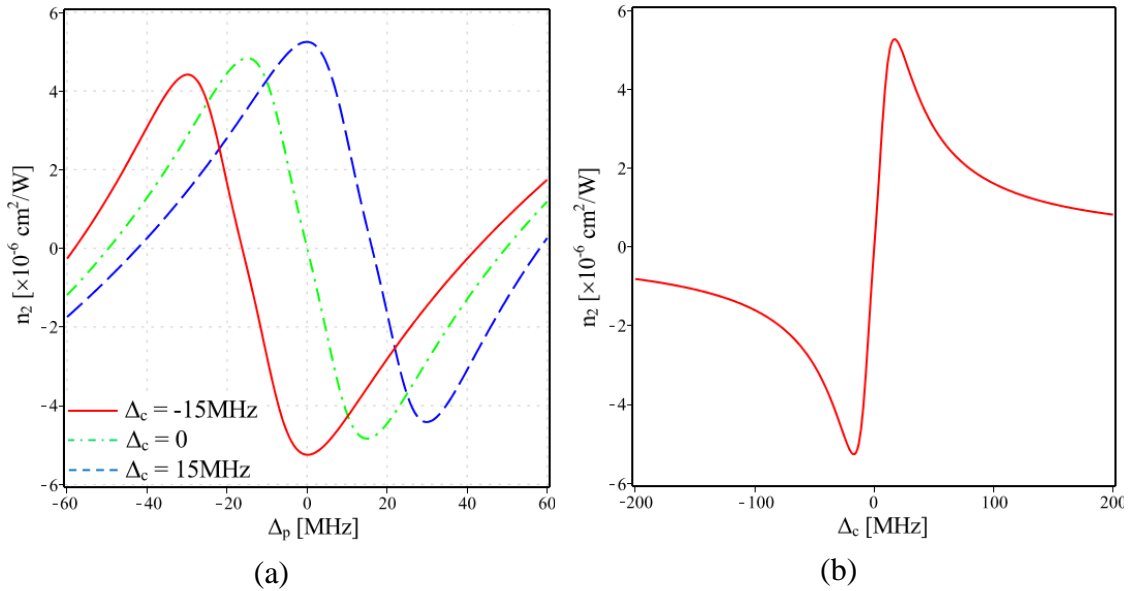

(a)   (b)

Figure 4. (a) The Kerr nonlinear coefficient as a function of probe detuning with different values of coupling detuning $\Delta_c = 0$ (dash-dotted line), $\Delta_c = 15$ MHz (dashed line), and $\Delta_c = -15$ MHz (solid line); (b) The Kerr nonlinear coefficient as a function of coupling detuning when $\Delta_p = 0$

Note: Other parameters are taken as $\Omega_c = 100$ MHz and $T = 300$ K.

In Figure 4, we analyze the control of the Kerr nonlinear coefficient according to the frequency of the coupling field when the coupling intensity is fixed at $\Omega_c = 100$ MHz. Figure 4(a) shows the variations of the Kerr nonlinear coefficient with probe detuning Δ_p for different values of the coupling detuning $\Delta_c = 0$ (dash-dotted line), $\Delta_c = -15$ MHz (solid line), and $\Delta_c = 15$ MHz (dashed line). We can see that a zero point for the Kerr nonlinear coefficient at the probe resonant frequency $\Delta_p = 0$ in the case of $\Delta_c = 0$ is transformed into a positive peak or negative peak when $\Delta_c = 15$ MHz or $\Delta_c = -15$ MHz, respectively. The change of the Kerr nonlinear coefficient with the coupling detuning when $\Delta_p = 0$ and $\Omega_c = 100$ MHz is presented in Figure 4(b). It shows that the variation of the Kerr nonlinear coefficient with the coupling detuning is similar to the variation of the

Kerr nonlinear coefficient with the probe detuning. That is, it also has a pair of negative-positive peaks of the Kerr nonlinear coefficient around the resonant frequency of the coupling field $\Delta_c = 0$. When the coupling frequency goes away from the atomic resonant frequency, the amplitude of the Kerr nonlinear coefficient decreases rapidly to zero. This is because the Kerr nonlinear coefficient is only enhanced in the EIT spectral domain when the condition of two-photon resonance is established ($\Delta_p = \Delta_c = 0$). The sign of the nonlinear coefficient can also be changed by adjusting the coupling frequency to the short or long wavelength domain.

Finally, we analyze the dependence of the Kerr nonlinear coefficient on temperature by plotting the Kerr nonlinear coefficient versus probe detuning Δ_p for various temperatures $T = 100$ K (solid line), $T = 200$ K (dashed line), and $T = 300$ K (dash-dotted line), as illustrated in Figure 5(a). The variations of the Kerr nonlinear coefficient with temperature when $\Omega_c = 100$ MHz, $\Delta_c = 0$, $\Delta_p = 10$ MHz (solid line), and $\Delta_p = -10$ MHz (dashed line) are shown in Figure 5(b). From the figure we can see that the profile of the nonlinear coefficient is greatly broadened and its amplitude is remarkably reduced when the temperature increases.
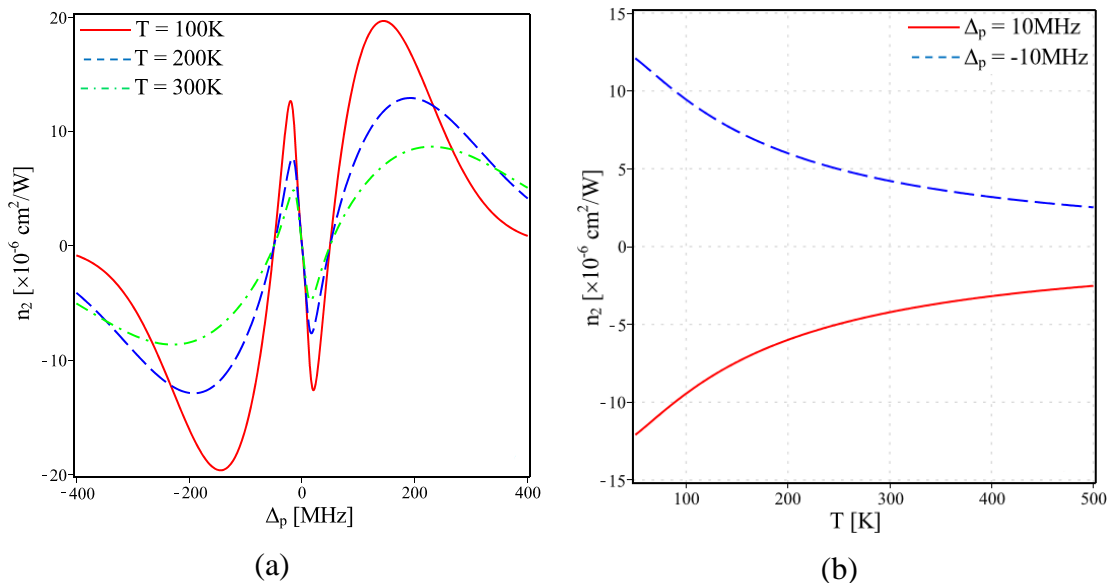

(a)   (b)

Figure 5. (a) The Kerr nonlinear coefficient as a function of probe detuning for different temperatures $T = 100$ K (solid line), $T = 200$ K (dashed line), and $T = 300$ K (dash-dotted line); (b) The Kerr nonlinear coefficient as a function of temperature for different values of probe detuning $\Delta_p = -10$ MHz (dashed line) and $\Delta_p = 10$ MHz (solid line)

Note: Other parameters are taken as $\Delta_c = 0$ and $\Omega_c = 100$ MHz.

4.   CONCLUSION

We have analyzed the enhancement and control of the self-Kerr nonlinear coefficient in a three-level V-type inhomogeneously broadened atomic medium by the analytical method. The study results have shown that the Kerr nonlinear coefficient is

enhanced considerably under the EIT condition. By adjusting the intensity or frequency of the coupling field, the magnitude and sign of the Kerr nonlinear coefficient are also changed significantly. The amplitude of the Kerr nonlinear coefficient decreases remarkably as temperature increases (i.e., the Doppler width increases). We note that the relaxation rate between excited states in the V-type scheme is much greater than that in the lambda-type scheme; therefore, the enhancement of the Kerr nonlinear coefficient occurs at a stronger coupling intensity. The analytical model can find potential applications in photonic devices and can explain the experimental observations of the Kerr nonlinear coefficient at different temperatures.

ACKNOWLEDGMENTS

REFERENCES

Anton, M. A., & Calderon, O. G. (2002). Optical bistability using quantum interference in V-type atoms. *Journal of Optics B: Quantum and Semiclassical Optics, 4*, 91-98.

Bai, Y., Guo, H., Han, D., & Sun, H. (2005). Effects of spontaneously generated coherence on the group velocity in a V system. *Physical Letters A, 340*(1-4), 342-346.

Bai, Y., Guo, H., Sun, H., Han, D., Liu, C., & Chen, X. (2004). Effects of spontaneously generated coherence on the conditions for exhibiting lasing without inversion in a V system. *Physical Review A, 69*, 1-5.

Bai, Y., Liu, T., & Yu, X. (2012). Giant Kerr nonlinearity in an open V-type system with spontaneously generated coherence. *Optik, 124*(7), 613-616.

Bang, N. H., Doai, L.V., & Khoa, D. X. (2019). Controllable optical properties of multiple electromagnetically induced transparency in gaseous atomic media. *Communications in Physics, 29*(1), 1-33.

Bang, N. H., Khoa, D. X., Son, D. H., & Doai, L. V. (2019). Effect of Doppler broadening on giant self-Kerr nonlinearity in a five-level ladder-type system. *Journal of the Optical Society of America B, 36*(11), 3151-3158.

Boller, K. J., Imamoglu, A., & Harris, S. E. (1991). Observation of electromagnetically induced transparency. *Physical Review Letters, 66*, 2593-2596.

Boyd, R. W. (2008). *Nonlinear optics*. Academic Press.

Doai, L. V. (2019). Giant cross-Kerr nonlinearity in a six-level inhomogeneously broadened atomic medium. *Journal of Physics B: Atomic, Molecular and Optical Physics, 52*, 1-9.

Doai, L. V., Khoa, D. X., & Bang, N. H. (2015). EIT enhanced self-Kerr nonlinearity in the three-level lambda system under Doppler broadening. *Physica Scripta, 90*(4), 1-6.

Fleischhauer, M., Imamoglu, I., & Marangos, J. P. (2005). Electromagnetically induced transparency: Optics in coherent media. *Reviews of Modern Physics, 77*, 633-673.

Gao, H., Sun, H., Fan, S., & Zhang, H. (2016). Phase control of Kerr nonlinearity in V-type system with spontaneously generated coherence. *Journal of Modern Optics, 63*(6), 598-604.

Hamedi, H. R., Gharamaleki, A. H., & Sahrai, M. (2016). Colossal Kerr nonlinearity based on electromagnetically induced transparency in a five-level double-ladder atomic system. *Applied Optics, 55*(22), 5892-5899.

Hamedi, H. R., & Juzeliunas, G. (2015). Phase-sensitive Kerr nonlinearity for closed-loop quantum systems. *Physical Review A, 91*, 1-13.

Han, D., Zeng, Y., Bai, Y., Chen, W., & Lu, H. (2007). Phase effects on group velocity propagation in a V-type system with spontaneously generated coherence. *Journal of Modern Optics, 54*, 493-500.

Harris, S. E., Field, J. E., & Imamoglu, A. (1990). Nonlinear optical processes using electromagnetically induced transparency. *Physical Review Letters, 64*, 1107-1110.

Harris, S. E., & Hau, L. V. (1995). Nonlinear optics at low light levels. *Physical Review Letters*, *82*, 4611-4614.

Joshi, A., Yang, W., & Xiao, M. (2003). Effect of quantum interference on optical bistability in the three-level V-type atomic system. *Physical Review A, 68*, 1-4.

Khoa, D. X., Doai, L. V., Son, D. H., & Bang, N. H. (2014). Enhancement of self-Kerr nonlinearity via electromagnetically induced transparency in a five-level cascade system: An analytical approach. *Journal of the Optical Society of America B, 31*(6), 1330-1334.

Li, J. (2007). Coherent control of optical bistability in a microwave-driven V-type atomic system. *Physica D: Nonlinear Phenomena*, *228*(2), 148-152.

Li, Y.-q., & Xiao, M. (1995a). Electromagnetically induced transparency in a three-level Λ-type system in rubidium atoms. *Physical Review A, 51*(4), 2703-2706.

Li, Y.-q., & Xiao, M. (1995b). Electromagnetically induced transparency in ladder-type inhomogeneously broadened media: Theory and experiment. *Physical Review A, 51*(1), 576-584.

Mousavi, S. M., Safari, L., Mahmoudi, M., & Sahrai, M. (2010). Effect of quantum interference on the optical properties of a three-level V-type atomic system beyond the two-photon resonance condition. *Journal of Physics B: Atomic, Molecular and Optical Physics, 43*, 1-8.

Sheng, J., Yang, X., Wu, H., & Xiao, M. (2011). Modified self-Kerr-nonlinearity in a four-level N-type atomic system. *Physical Review A, 84*, 1-5.

Wang, H., Goorskey, D., & Xiao, M. (2001). Enhanced Kerr nonlinearity via atomic coherence in a three-level atomic system. *Physical Review Letters, 87*(7), 1-4.

Zhao, J., Wang, L., Xiao, L., Zhao, Y., Yin, W., & Jia, S. (2002). Experimental measurement of absorption and dispersion in V-type cesium atom. *Optics Communications, 206*, 341-345.